A Dual Reciprocity Method for a Class of Heat Conduction Problems in Two-Layered Materials

Imam Solekhudin*, Moh. Ivan Azis

***Abstract*—In this paper, problems involving steady heat conduction in two-layered materials are considered. The problems are governed by diffusion equations. These equations may be solved analytically for a limited number of problems. Hence, a numerical method is needed to solve these problems. In this paper, a numerical method known as the Dual Reciprocity Method (DRM) is employed to solve the problems numerically. To test the accuracy of the numerical method, three problems with analytical solutions are solved numerically using the DRM. Comparisons between numerical and corresponding analytical solutions are presented and discussed. Moreover, problems with unknown analytical solutions are solved numerically by employing the method. Some numerical results are presented to verify the effect of material diversity to the heat conduction.**

***Index Terms*—Heat conduction, dual reciprocity method, steady diffusion equation, two-layered materials.**

I. Introduction

HEAT conduction problems have been studied by numerous researchers. Such researchers are Fu et al. [1], Bao et al. [2], Xu et al. [3], Azis et al. [4], and Pramesti et al. [5]. In these studies, many types of materials have been considered, such as Functionally Graded Materials (FGMs) and porous media. Some researchers also studied heat conduction in layered materials. Among the researchers studied layered materials are Gao et. al. [7] Di et al., Johansson and Lesnic [8], and Qiu et. al. [9].

Recently, researchers have been working on heat conduction in layered materials, experimentally or numerically. Gao et al. reviewed progress, challenges, and perspectives in the design and application of 2D layered material (2DLM) for nanofluidic research conducted experimentally [7]. Johansson and Lesnic conducted numerical studies by applying a fundamental solution method for solving problems involving transient heat conduction in layered materials [8]. The problems in [8] are also solved numerically using a meshless singular boundary method [9]. In the numerical studies that have been carried out by these researchers, the heat conduction problems studied do not involve a source term. Hence, we presume that it is necessary to continue their studies by involving a source term. As in real life situation, sometimes a source is generated inside the materials.

The heat conduction problems considered in this paper may be solved numerically using the Dual Reciprocity Method (DRM), a method that has been widely used by researchers to solve numerous problems numerically. Some of such problems are convection-diffusion-reaction problems ([10], [11], and [12]), infiltration problems ([13], [17], [15], [16], [17], [18], and [19]), and crack problems ([20], [21], and [22]).

In this study, we extend the problems investigated in [8] and [9] by incorporating a source generated in the materials. For the completion of our paper and the convenience of readers, the mathematical formulation, involving problem formulation and method of solution (DRM), is presented. We also present several problems with analytical solutions to test the DRM. The DRM is then employed to solve some heat conduction problems with unknown analytical solutions. Two set of problems are considered. Numerical results are presented and analyzed to determine the influence of layered materials on the temperature distribution inside the material.

Manuscript received January 18, 2022; revised December 07, 2022.

*Corresponding author. Imam Solekhudin is a Professor at Department of Mathematics, Faculty of Mathematics and Natural Sciences, Universitas Gadjah Mada, Yogyakarta, INDONESIA. Email: imams@ugm.ac.id

Moh. Ivan Azis is a Professor at Department of Mathematics, Faculty of Mathematics and Natural Sciences, Universitas Hasanuddin, INDONESIA. Email: ivan@unhas.ac.id

II. Problem formulation and basic equations

We consider two-layered materials consisting of upper layer and lower layer. Each layer is an isotropic homogeneous material. The regions of upper layer and lower layer are denoted as R_1 and R_2, respectively. These regions are defined as

$$R_1 = \{(x,y) : 0 \le x \le L, \text{ and } 0 \le y \le K\}, \quad (1)$$

$$R_2 = \{(x,y) : 0 \le x \le L, \text{ and } -K \le y \le 0\}, \quad (2)$$

where $L, K > 0$. An illustration of the two-layered material is shown in Figure 1.

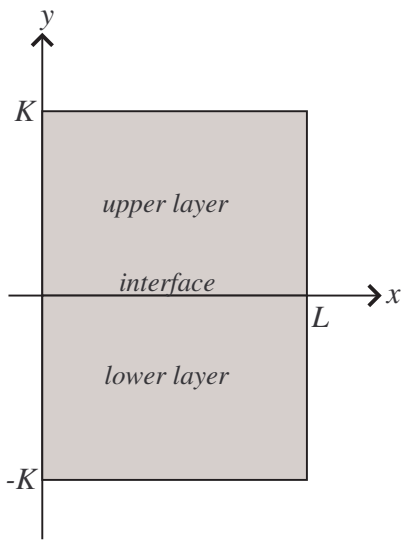

Fig. 1: Two-layered materials considered in this study.

Problems involving heat conduction in two-layered

isotropic materials are governed by a system of equations

$$\rho_1 c_1 \frac{\partial T_1}{\partial t} = D_1 \left(\frac{\partial^2 T_1}{\partial x^2} + \frac{\partial^2 T_1}{\partial y^2} \right) + G_1(x,y), \quad (3)$$

$$\rho_2 c_2 \frac{\partial T_2}{\partial t} = D_2 \left(\frac{\partial^2 T_2}{\partial x^2} + \frac{\partial^2 T_2}{\partial y^2} \right) + G_2(x,y), \quad (4)$$

where T_1 is the temperature in the upper layer, T_2 is the temperature in the lower layer, ρ_1 is the mass density of the upper layer material, ρ_2 is the mass density of the lower layer material, c_1 is the specific heat of the upper layer material, c_2 is the specific heat of the lower layer material, D_1 and D_2 are, respectively, the thermal conductivity of the upper layer and the lower layer materials, G_1 is the source generated in the upper layer, and G_2 is the source generated in the lower layer.

Interface conditions are given by

$$T_1 = T_2, \quad (5)$$

$$F_1 = -F_2, \quad (6)$$

where

$$F_1 = D_1 \frac{\partial T_1}{\partial n}, \quad (7)$$

$$F_2 = D_2 \frac{\partial T_2}{\partial n}, \quad (8)$$

respectively. For the case of steady heat conduction problems, the system of equations (3) and (4) can be expressed as follows.

$$\frac{\partial^2 T_1}{\partial x^2} + \frac{\partial^2 T_1}{\partial y^2} + g_1(x,y) = 0, \quad (9)$$

$$\frac{\partial^2 T_2}{\partial x^2} + \frac{\partial^2 T_2}{\partial y^2} + g_2(x,y) = 0, \quad (10)$$

where

$$g_1(x,y) = \frac{G_1(x,y)}{D_1} \text{ and } g_2(x,y) = \frac{G_2(x,y)}{D_2}.$$

To implement the DRM, similar to those in [23] and [24], the solutions of Equation (9) and Equation (10) are expressed as integral equations

$$\lambda(\xi_1,\eta_1) T_1(\xi_1,\eta_1) = \iint_{R_1} \tau(x,y;\xi_1,\eta_1) g_1(x,y) dx\, dy + \int_{C_1} \left[T_1(x,y) \frac{\partial}{\partial n} \Big(\tau(x,y;\xi_1,\eta_1) \Big) - \tau(x,y;\xi_1,\eta_1) \frac{\partial}{\partial n} \Big(T_1(x,y) \Big) \right] ds, \quad (11)$$

$$\lambda(\xi_2,\eta_2) T_2(\xi_2,\eta_2) = \iint_{R_2} \tau(x,y;\xi_2,\eta_2) g_2(x,y) dx\, dy + \int_{C_2} \left[T_2(x,y) \frac{\partial}{\partial n} \Big(\tau(x,y;\xi_2,\eta_2) \Big) - \tau(x,y;\xi_2,\eta_2) \frac{\partial}{\partial n} \Big(T_2(x,y) \Big) \right] ds, \quad (12)$$

where C_1 and C_2 are, the boundary of R_1 and R_2, respectively,

$$\lambda(\xi_i,\eta_i) = \begin{cases} 1/2 & , \text{ if } (\xi_i,\eta_i) \text{ on smooth part of } C_i \\ 1 & , \text{ if } (\xi_i,\eta_i) \in R_i \end{cases}, \quad i = 1,2.$$

and

$$\tau(x,y;\xi,\eta) = \frac{1}{4\pi} \ln[(x-\xi)^2 + (y-\eta)^2]$$

is the fundamental solution of two-dimensional Laplace equation.

Integral equations (11) and (12) may be recast into a system of linear algebraic equations by applying the algorithm in [6].

III. Test Problems with Analytic Solution

In this section, the method presented in Section II is tested for accuracy. Three problems with analytic solutions, namely Problem 1, Problem 2, and Problem 3 are presented.

A. Problem 1

In Problem 1, we consider a system of equations involving Equation (9) and Equation (10), where

$$g_1(x,y) = -2(x^2+y^2), \quad (13)$$

$$g_2(x,y) = -2xe^{y^2}(2y^4+5y^2+1), \quad (14)$$

with Dirichlet boundary conditions

$$T_1 = y^2, \text{ for } x = 1 \text{ and } 0 < y < 1, \quad (15)$$

$$T_1 = x^2, \text{ for } 0 < x < 1 \text{ and } y = 1, \quad (16)$$

$$T_1 = 0, \text{ for } x = 0 \text{ and } 0 < y < 1, \quad (17)$$

$$T_2 = 0, \text{ for } x = 0 \text{ and } -1 < y < 0, \quad (18)$$

$$T_2 = xe, \text{ for } 0 < x < 1 \text{ and } y = -1, \quad (19)$$

$$T_2 = y^2 e^{y^2}, \text{ for } x = 1 \text{ and } -1 < y < 0. \quad (20)$$

In this problem, we set $D_1 = D_2$.

Problem 1 have analytic solutions,

$$T_1 = x^2 y^2, \text{ for } 0 \le x \le 1 \text{ and } 0 \le y \le 1 \quad (21)$$

and

$$T_2 = xy^2 e^{y^2}, \text{ for } 0 \le x \le 1 \text{ and } -1 \le y \le 0. \quad (22)$$

The DRM is then implemented to solve Problem 1 using two sets of boundary elements and interior collocation points. The two sets are named as Set A and Set B, which are summarized in Table I. Some of the results obtained are presented in Table II, Figure 2 and Figure 3.

TABLE I: Sets of boundary elements and interior collocation points.

Set name	Number of boundary element	Number of interior collocation point
Set A	320	361 (19×19)
Set B	400	361 (19×19)

Table II shows numerical solutions, analytical solutions and absolute errors, at selected points. From Table II, it can be seen that, generally, Set B yields more accurate solutions, as Set B has more number of elements than Set A. At the

TABLE II: Numerical and analytical solutions at selected points

Layer	Point	Num. (Set A)	Num. (Set B)	Analytic	e_A	e_B
Upper layer	$(0.05, 0.05)$	0.00072623	0.00020887	0.00000625	0.00071998	0.00020262
	$(0.05, 0.50)$	0.00060032	0.00062947	0.00062500	0.00002468	0.00000447
	$(0.05, 0.95)$	0.00223510	0.00225766	0.00225625	0.00002115	0.00000141
	$(0.50, 0.50)$	0.06238915	0.06261535	0.06250000	0.00011085	0.00011535
	$(0.95, 0.05)$	0.00412022	0.00360824	0.00225625	0.00186397	0.00135199
	$(0.95, 0.50)$	0.22576261	0.22566774	0.22562500	0.00013761	0.00004274
	$(0.95, 0.95)$	0.81352004	0.81451156	0.81450625	0.00098621	0.00000531
Lower layer	$(0.05, -0.05)$	0.00078766	0.00029686	0.00012531	0.00066235	0.00017155
	$(0.05, -0.50)$	0.01557977	0.01585311	0.01605032	0.00047055	0.00019721
	$(0.05, -0.95)$	0.11113849	0.11126423	0.11126741	0.00012892	0.00000318
	$(0.50, -0.50)$	0.15998066	0.16060390	0.16050318	0.00052252	0.00010072
	$(0.95, -0.05)$	0.00450773	0.00377192	0.00238094	0.00212679	0.00139098
	$(0.95, -0.50)$	0.30440096	0.30495372	0.30495604	0.00055508	0.00000232
	$(0.95, -0.95)$	2.11138382	2.11405268	2.11408082	0.00269700	0.00002814

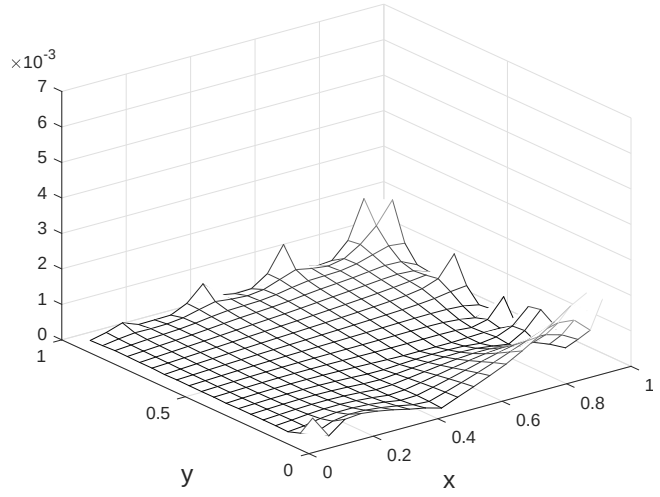

(a) Upper layer

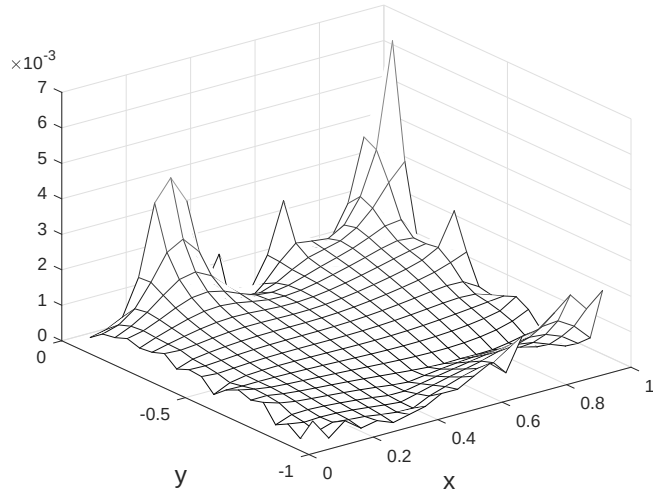

(b) Lower layer

Fig. 2: Mesh plots of absolute errors for Problem 1 using Set A.

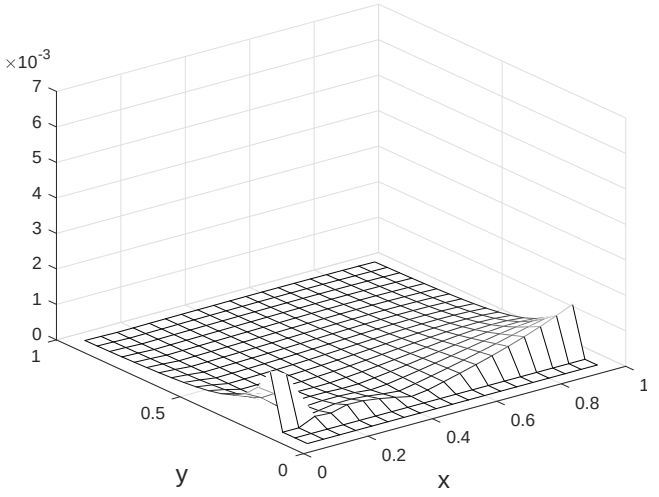

(a) Upper layer

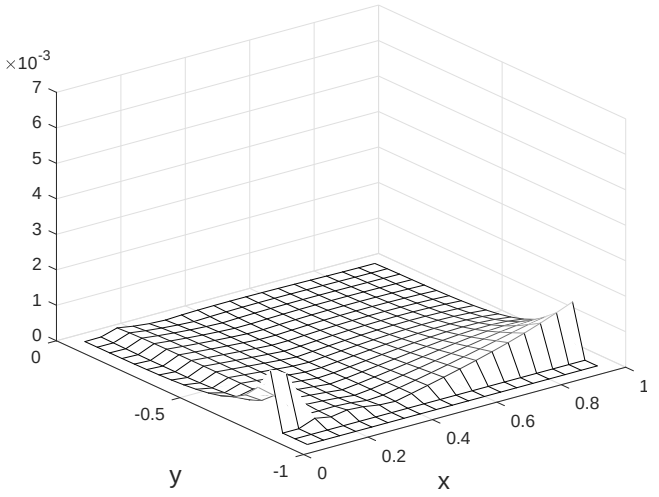

(b) Lower layer

Fig. 3: Mesh plots of absolute errors for Problem 1 using Set B.

selected points, the absolute errors resulted from Set A and Set B are less than 2.7×10^{-3} and 1.4×10^{-3}, respectively.

Distribution of the absolute errors over the domain can be observed in Figure 2 and Figure 3. From Figure 2, the maximum value of absolute error resulted from Set A is achieved at the interface. More specifically, the maximum value of the absolute error is about 6×10^{-3}, at point $(1, 0)$. Figure 3 shows the distribution of the absolute errors attained from Set B. In most part of the domain, the resulting absolute errors are close to 0, except on some area, for instance at $(0, 0.2)$, $(1, 0.2)$, $(0, -0.8)$ and $(1, -0.8)$. The maximum value of the absolute errors is observed at around 1×10^{-3}. From the results presented in Table II, Figure 2, and Figure 3, we may conclude that, generally, Set B results in more accurate numerical solutions than Set A.

For the objective of error assessment, we calculate the

average total absolute error (ATAE) along lines $x = 0.05 \times k,\ k = 1, 2, \cdots, 19$. For each line, the total absolute error (TAE) is computed using formula

$$TAE = \frac{1}{2}\int_{-1}^{1} AE\ dy, \tag{23}$$

where AE is the absolute error. Here, we may not apply the relative error as the analytic solution at $y = 0$ is 0. We employ the Simpson's Rule to compute the integral in (23), with 20 subdivisions for each layer. The average of the total absolute error is calculated by taking the mean of the total relative error along the 19 distinct lines. The results are presented in Table III.

TABLE III: ATAE resulted from Set A and Set B.

Set name	ATAE
Set A	4.9×10^{-3}
Set B	1.6×10^{-3}

From Table III, we may infer that Set B is about 3 times more accurate than Set A. Nevertheless, from the results obtained, DRM gives accurate solutions. Therefore, by considering the accuracy and efficiency, henceforth, the DRM is implemented using Set A, as Set A needs less computational times than Set B.

B. Problem 2

In this subsection, we consider a system of equations involving Equation (9) and Equation (10), where

$$\begin{aligned} g_1(x,y) &= e^x[2\pi^2\cos^2(\pi y) \\ &\quad +(1-2\pi^2)\sin^2(\pi y)], \qquad (24)\\ g_2(x,y) &= 6-2x, \qquad (25)\end{aligned}$$

with Robin boundary conditions

$$\begin{aligned} T_1 &= e\sin^2(\pi y),\ \text{for } x=1 \text{ and } 0<y<1, \qquad (26)\\ \frac{\partial T_1}{\partial n} &= 0,\ \text{for } 0<x<1 \text{ and } y=1, \qquad (27)\\ T_1 &= \sin^2(\pi y),\ \text{for } x=0 \text{ and } 0<y<1, \qquad (28)\\ T_2 &= 3y^2,\ \text{for } x=0 \text{ and } -1<y<0, \qquad (29)\\ \frac{\partial T_2}{\partial n} &= 2(3-x),\ \text{for } 0<x<1 \text{ and } y=-1, \qquad (30)\\ T_2 &= 2y^2,\ \text{for } x=1 \text{ and } -1<y<0. \qquad (31)\end{aligned}$$

As those in Problem 1, the values of D_1 and D_2 satisfy $D_1 = D_2$.

The analytic solutions to Problem 2 are

$$T_1 = e^x\sin^2(\pi y),\ \text{for } 0\le x\le 1 \text{ and } 0\le y\le 1, \tag{32}$$

and

$$T_2 = y^2(3-x),\ \text{for } 0\le x\le 1 \text{ and } -1\le y\le 0. \tag{33}$$

Problem 2 is solved numerically using the DRM by discretizing the boundary into 320 elements, and 361 interior collocation points are chosen. The graphs of numerical solutions obtained using the DRM with their corresponding analytic solutions can be seen in Figure 4.

Figure 4, shows the numerical results and corresponding analytical results at four different lines. As can be observed in Figure 4, the numerical results obtained using the DRM are in good accuracy with the corresponding analytical solutions. Using the error measurement as that in Problem 1, the value of ATAE is 8.1×10^{-3}. This shows that the numerical solutions have good agreements with the corresponding analytical solutions.

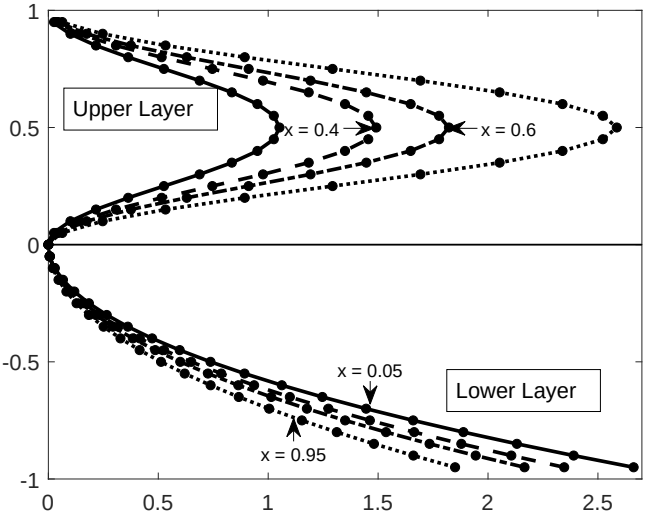

Fig. 4: Temperature (T) profile for Problem 2, compared with the analytic solutions (represented with dots).

C. Problem 3

In Problem 3, a system of equations involving Equation (9) and Equation (10), where

$$\begin{aligned} g_1(x,y) &= \pi^2(x^2+y^2)\sin(\pi xy), \qquad (34)\\ g_2(x,y) &= 4\pi^2(x^2+y^2)\sin(2\pi xy), \qquad (35)\end{aligned}$$

are considered. The boundary conditions of the problem are

$$\begin{aligned} \frac{\partial T_1}{\partial n} &= 2\pi y\cos(\pi y),\ \text{for } x=1 \text{ and } 0<y<1, \qquad (36)\\ T_1 &= 2\sin(\pi x),\ \text{for } 0<x<1 \text{ and } y=1, \qquad (37)\\ T_1 &= 0,\ \text{for } x=0 \text{ and } 0<y<1, \qquad (38)\\ T_2 &= 0,\ \text{for } x=0 \text{ and } -1<y<0, \qquad (39)\\ T_2 &= -2\sin(2\pi x),\ \text{for } 0<x<1 \text{ and } y=-1, \qquad (40)\\ \frac{\partial T_2}{\partial n} &= 4\pi y\cos(2\pi y),\ \text{for } x=1 \text{ and } -1<y<0. \qquad (41)\end{aligned}$$

Here, the values of D_1 and D_2 satisfy $D_1 = 2D_2$. The analytic solutions of the problem are

$$T_1 = \sin(\pi xy),\ \text{for } 0\le x\le 1 \text{ and } 0\le y\le 1, \tag{42}$$

and

$$T_2 = \sin(2\pi xy),\ \text{for } 0\le x\le 1 \text{ and } -1\le y\le 0. \tag{43}$$

Using the DRM with 320 line segments and 361 interior collocation points, as those in Problem 2, the numerical results are obtained. The graphs of numerical solutions with their corresponding analytic solutions are presented in Figure 5.

As that in Problem 2, Figure 5 shows the numerical solutions and the corresponding analytical solutions for Problem 3. Compared to the two previous problems, there is a

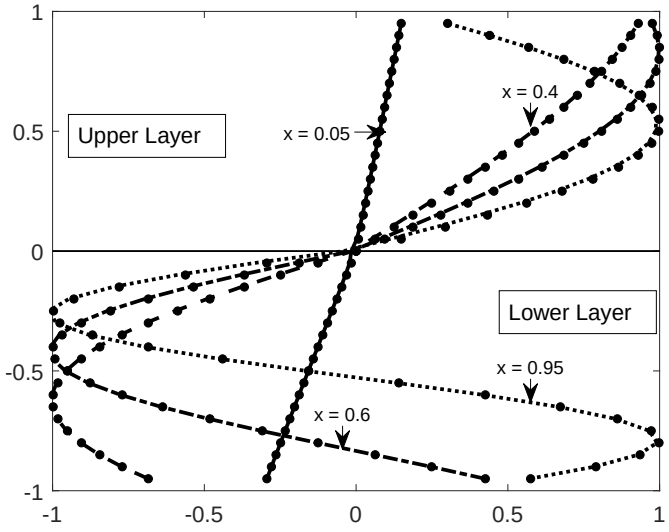

Fig. 5: Temperature (T) profile for Problem 3, compared with the analytic solutions (represented with dots).

difference in the relation between D_1 and D_2. In Problem 1 and Problem 2, we set $D_1 = D_2$. In Problem 3, the value of D_1 is twice the value of D_2 ($D_1 = 2D_2$). As before, by observing Figure 5, it is seen that the numerical solutions obtained have a good accuracy. The value of ATAE is 6.8×10^{-2}.

IV. Problems without Analytic Solution

In this section we consider a system of equations involving Equation (9) and Equation (10) with unknown analytic solutions. There are two sets of problems considered. The sets of problems are as follows.

A. Set of Problems 1

In the set of problems 1, we consider cases with $D_1 = D_2$. There are four different cases considered, named as Case A, Case B, Case C, and Case D. In this set of problems, we investigate influences of sources placed at a part of boundary and inside the materials. Sources generated inside Layer 1 and Layer 2 are governed by functions g_1 and g_2, respectively. The source at the part of boundary is governed by function u. Functions g_1, g_2, and u for the four cases considered are summarized in Table IV.

TABLE IV: Source g_1, g_2, and u for four different cases.

Case	$g_1(x,y)$	$g_2(x,y)$	$u(x,y)$
Case A	$400y(1-y)$	$-400y(1+y)$	$100-\lvert 200(x-\frac{1}{2})\rvert$
Case B	$100(1-y^2)$	$100(1-y^2)$	$100-\lvert 200(x-\frac{1}{2})\rvert$
Case C	$100(1-y^2)$	$100(1-y^2)$	$-400x(x-1)$
Case D	$400y(1-y)$	$-400y(1+y)$	$-400x(x-1)$

The boundary conditions of the problems are Dirichlet boundary conditions as follows.

$$T_1 = 0, \text{ for } x = 1 \text{ and } 0 < y < 1, \quad (44)$$

$$T_1 = u(x,y), \text{ for } 0 < x < 1 \text{ and } y = 1, \quad (45)$$

$$T_1 = 0, \text{ for } x = 0 \text{ and } 0 < y < 1, \quad (46)$$

$$T_2 = 0, \text{ for } x = 0 \text{ and } -1 < y < 0, \quad (47)$$

$$T_2 = 0, \text{ for } 0 < x < 1 \text{ and } y = -1, \quad (48)$$

$$T_2 = 0, \text{ for } x = 1 \text{ and } -1 < y < 0. \quad (49)$$

This set of problems are solved using the DRM with 320 elements and 361 interior collocation points. The numerical results obtained are presented in Figure 6 - Figure 7.

Figure 6 shows the graphs of T at three different values of x. From the functions g_1, g_2 and u given in Table IV, and the boundary conditions (44) - (49), the problems to solve are symmetrical about the line $x = 0.5$. Hence, the three values of x in Figure 6 must be less than or equal to 0.5. The three values of x are $x = 0.1$, $x = 0.3$, and $x = 0.5$. From Figure 6, it can be observed that the values of T in Case C and Case D are higher than those in Case A and Case B. These mean that the source $u(x,y) = -400x(x-1)$ results in higher temperature compared to the source $u = 100 - |200(x - \frac{1}{2})|$. These may be affected by the total source at $y = 0$, as

$$\int_0^1 -400x(x-1)dx = \frac{200}{3} > 50 = \int_0^1 \left[100 - \left|200\left(x - \frac{1}{2}\right)\right|\right] dx.$$

It can also be observed that the pair $g_1 = 400y(1-y)$ and $g_2 = -400y(1+y)$ produces in more curved graphs of T compared to the pair $g_1 = g_2 = 100(1-y^2)$. These results may be due to the first pair g_1 and g_2 being more curved than the second pair.

Figure 7 shows the distribution of temperature in the domain. It can be seen that the maximum temperature is gained at point $(0.5, 1)$. This is expected, as the function u reaches it's maximum value at this point. Observing Figure 7(a) and Figure 7(b), it can be seen that from $y = 0.5$ to $y = 1.0$, the distributions of temperature of Case A and Case B are about the same. A similar fashion also occurs for Case C and Case D. Moreover, comparing Figure 7(a) and Figure 7(c), it can be seen that the temperature at $y = 1$ for Case C is higher than that in Case A.

For the amount of total temperature, in all cases we use formula

$$\int_{-1}^{1}\int_{0}^{1} T(x,y)dxdy. \quad (50)$$

Since T is obtained numerically, the integral in (50) cannot be evaluated analytically. Thus, a numerical scheme is employed to estimate this integral. To compute the integral numerically, the domain is divided into 50×100 rectangular regions. Let A_{lk} be the region at k-th row and l-th column, and Δx_l and Δy_k be the breadth and the length of region A_{lk}, respectively.

Let T_{lk} be the numerical value of temperature T at one corner of A_{lk}. Now, the integral in (50) may be approximated using the formula

$$\sum_{l=1}^{50}\sum_{k=1}^{100} T_{lk}\Delta x_l \Delta y_k. \quad (51)$$

Using formula in (51), the numerical values of the total temperature on the domain are summarized in Table V.

From the results presented in Table V, we may conclude that the pair of heat source $g_1 = g_2 = 100(1-y^2)$ produces higher total temperature than the pair of heat source $g_1 = 400y(1-y)$ and $g_2 = -400y(1+y)$.

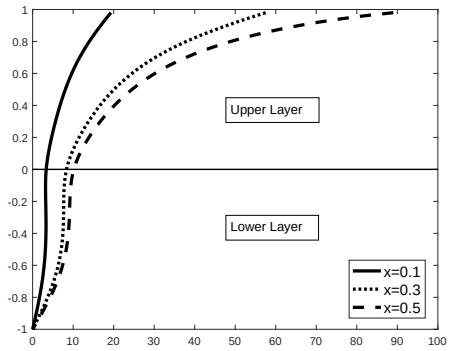

(a) Case A

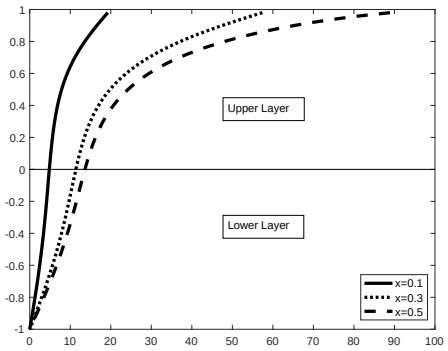

(b) Case B

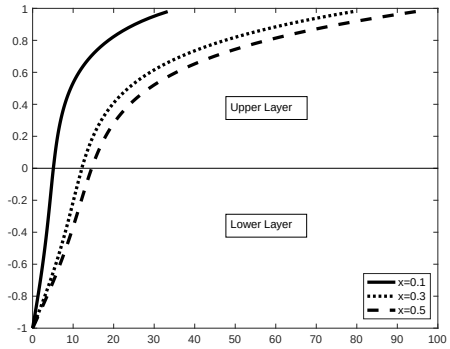

(c) Case C

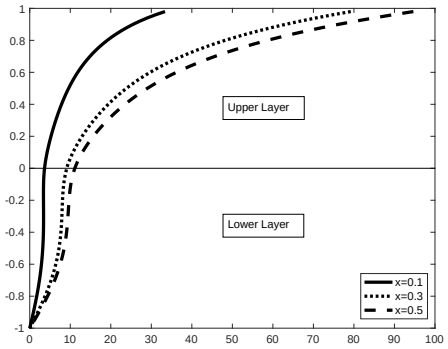

(d) Case D

Fig. 6: Plots of T vs y for selected values of x.

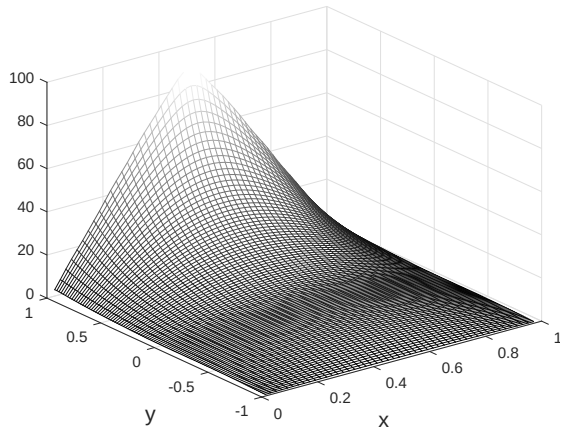

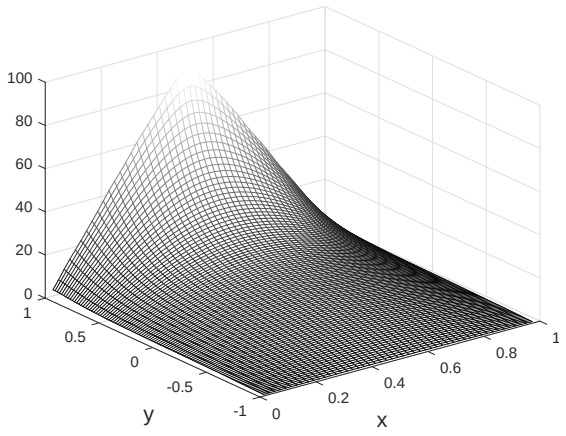

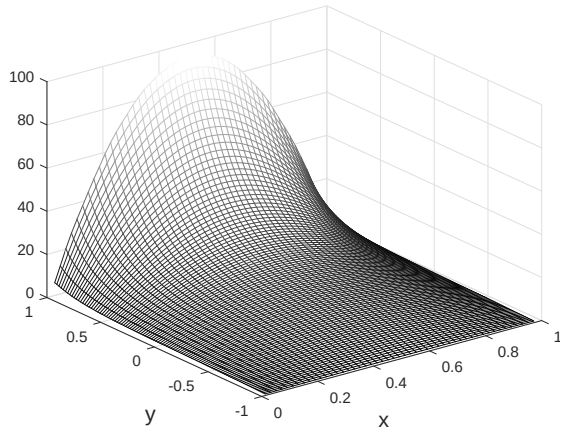

(c) Case C

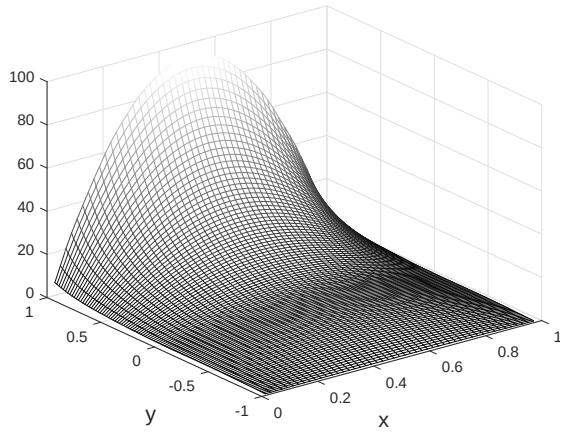

(d) Case D

Fig. 7: Surface plots of solutions over the region for the four different cases.

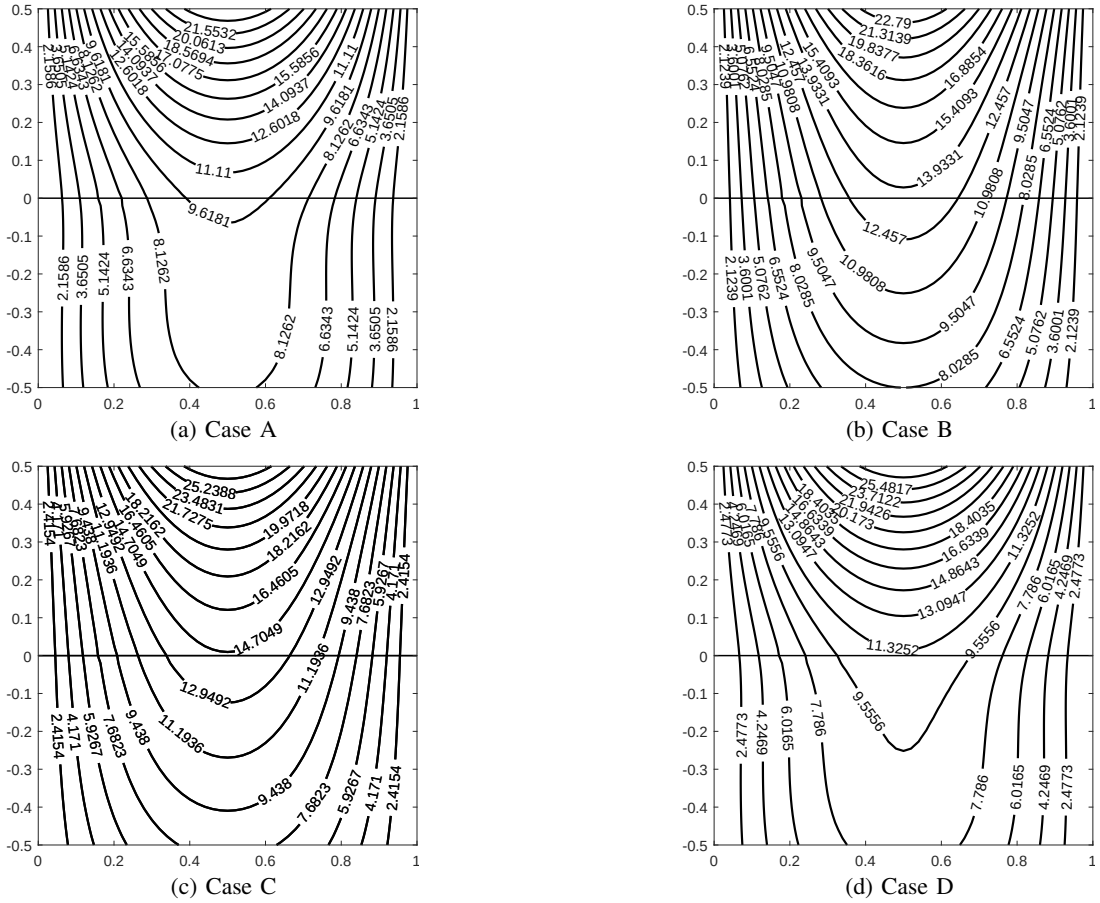

(a) Case A (b) Case B (c) Case C (d) Case D

Fig. 8: Contour plots of T for $-0.5 \leq y \leq 0.5$.

TABLE V: Total temperature from four different cases considered.

	Case A	Case B	Case C	Case D
Total T	23.83	24.57	29.16	28.42

Figure 8 shows contour plots of temperature T over region bounded by the set $\{(x, y) : 0 \leq x \leq 1 \text{ and } -0.5 \leq y \leq 0.5\}$. Here, the range of y is from -0.5 to 0.5. This range is needed to observe the distribution pattern of temperature on the area near the interface. There are four contour plots presented in Figure 8. From Figure 8(a) and Figure 8(b), although Case A and Case B have the same heat source u, the temperature resulted from Case B is higher than that resulted from Case A. For instance, the highest temperature at the interface in Case B is around 13.5, which is higher than that in Case A, which is about 10. This may be due to the fact that the total temperature generated in the range $-0.5 \leq y \leq 0.5$ in Case B is greater than that in Case A. The total temperature generated are $\frac{275}{3}$ and $\frac{200}{3}$, respectively. Furthermore, in the area shown in Figure 8, the temperature resulted from Case B has a range from 2 to 23, while the temperature resulted from Case A is ranged from 2 to 22.

A Similar fashion as that in Case A and Case B also occurs in Case D and Case C, respectively. Similar conclusions are also obtained when we compare Case C and Case D (see Figure 8(c) and Figure 8(d)). However, since the total temperature at boundary $\{(x, y) : 0 \leq x \leq 1 \text{ and } y = 1\}$ in Case C and Case D is larger than that in Case A and Case B, the resulting temperatures from Case C and Case D are greater than those from Case A and Case B. The range of temperature resulting from Case C and Case D are from about 2 to 27 and from about 2 to 26, respectively. From the results presented we may conclude that the higher the total temperature at boundary $\{(x, y) : 0 \leq x \leq 1 \text{ and } y = 1\}$, the higher the resulting temperature in the domain. The greater the total temperature generated in the range $-0.5 \leq y \leq 0.5$, the higher the resulting temperature on the area around the interface.

B. Set of Problems 2

In the set of problems 2, we consider cases with $D_1 \neq D_2$. The boundary conditions of the problems in this set are as those in the set of problems 1. The source u is defined as

$$u = -400x(x - 1).$$

The sources generated in the domain, G_1 and G_2, are set as follows.

$$G_1 = G_2 = 20. \tag{52}$$

In this set of problems, we consider four different cases, named as Case A, Case B, Case C, and Case D. Thermal conductivities, and $g_1 = \frac{G_1}{D_1}$ and $g_2 = \frac{G_2}{D_2}$ of these four cases are summarized in Table VI.

As those in the set of problems 1, here we solve the problems using the DRM with 320 elements and 361 interior points. Using the DRM, numerical results of the problems are obtained. Some of the numerical results are presented in Table VII, and Figure 9 and Figure 10.

Table VII shows the numerical values of temperature at the interface. For $D_2 = 3.0$ (Case A), the values of numerical

TABLE VI: Thermal conductivities D_1 and D_2, and functions g_1 and g_2 for four different cases.

Case	D_1	D_2	$g_1(x, y)$	$g_2(x, y)$
Case A	1.0	3.0	20	6.67
Case B	1.0	2.0	20	10
Case C	1.0	0.5	20	40
Case D	1.0	0.33	20	60

TABLE VII: Temperature at interface for four different cases of two-layered materials, and at $y = 0$ for homogeneous material.

Point	Case A	Case B	Isotropic Homogeneous Material	Case D	Case E
$(0.1, 0.0)$	21.63	28.84	43.26	57.69	64.90
$(0.2, 0.0)$	21.65	28.87	43.30	57.73	64.95
$(0.3, 0.0)$	21.67	28.90	43.35	57.80	65.02
$(0.4, 0.0)$	21.69	28.92	43.39	57.85	65.08
$(0.5, 0.0)$	21.70	28.94	43.40	57.87	65.10
$(0.6, 0.0)$	21.69	28.92	43.39	57.85	65.08
$(0.7, 0.0)$	21.67	28.90	43.35	57.80	65.02
$(0.8, 0.0)$	21.65	28.87	43.30	57.73	64.95
$(0.9, 0.0)$	21.63	28.84	43.26	57.69	64.90

temperature at the interface are about 21. In Case B and Case C ($D_2 = 2.0$ and $D_2 = 0.5$, respectively), the numerical values of T at the interface are about 28 and 57, respectively. The numerical values of temperature for $D_2 = 0.33$ (Case D) are around 65. These results indicate that the bigger the thermal conductivity in the lower layer, D_2, the lower the temperature at the interface.

The results presented in Table VII are the consequence of one of the conditions at the interface,

$$D_1 \frac{\partial T_1}{\partial n} = -D_2 \frac{\partial T_2}{\partial n},$$

which may be written as

$$\frac{D_1}{D_2} \frac{\partial T_1}{\partial n} = -\frac{\partial T_2}{\partial n}.$$

Since $D_1 = 1.0$ for all cases, then higher values of thermal conductivities in the lower layer, D_2, result in smaller values of $|\partial T_2/\partial n|$. Hence, higher values of D_2 result in smaller values of difference between the temperature at the interface and the temperature at $y = -1$.

Figure 9 shows the distribution of temperature over the domain for the isotropic homogeneous material and four different cases of layered materials. In particular, Figure 9(a) and Figure 9(b) show the distribution of temperature for Case A and Case B, respectively. The distribution of temperature over the isotropic homogeneous material is shown in Figure 9(c). The distribution of temperature for Case C and Case D can be seen in Figure 9(d) and Figure 9(e), respectively.

It can be seen that the maximum temperature is located at point $(0.5, 1)$. This is expected, as the maximum value of function $u = -400x(1 - x)$ defined over $\{(x, y) : 0 \leq x \leq 1 \text{ and } y = 1\}$ is achieved at that point. It can also be seen that the lower layer with smaller thermal conductivity yields higher temperature than those with higher thermal conductivities.

Figure 10 shows contour plots of temperature over area $\{(x, y) : 0 \leq x \leq 1 \text{ and } -0.5 \leq y \leq 0.5\}$. More specifically, Figure 10(a) and Figure 10(b) are contour plots resulted from Case A and Case B, respectively. Contour plots of temperature for the isotropic homogeneous material is shown in Figure 10(c). Figure 10(d) and Figure 10(e) show contour plots of temperature for Case C and Case D, respectively.

It can be seen that for Case A and Case B, a rapid decline in temperature in the upper layer from area located at $y = 0.5$ to area at $y = 0$ is observed. For Case A, the temperature drops from about 46 to 22. The decline in temperature for Case B is from about 49 to 29. On the other hand, in the lower layer from $y = 0$ to $y = -0.5$, the temperature decreases gradually from about 22 to 10 for Case A and from about 29 to 16 for Case B.

The opposite occurs for Case C and Case D. In the upper layer, the temperature declines gently. For Case C, temperature decreases from about 64 to 58. The decline in temperature for Case D is from about 68 to 66. In the lower layer, the temperature drops significantly from about 58 to 34 for Case C, and from about 66 to 40 for Case D.

These results indicate that the thermal conductivities of the materials affect the distribution of temperature over the domain considered. If the thermal conductivity of the upper layer is higher than that of the lower layer, then the temperature in the lower layer varies more than that in the upper layer. On the other hand, if the thermal conductivity of the upper layer is lower than that of the lower layer, then the temperature in the upper layer varies more than that in the lower layer.

V. Concluding remarks

Problems involving steady heat conduction in two-layered materials have been solved numerically using the DRM. The problems are solved by expressing the governing equations into integral equations. The resulted integral equations are then recast into a system of linear algebraic equations. By solving the linear algebraic equations, the required numerical solutions are obtained.

The method is tested using three problems with analytical solutions. The numerical results obtained are in good agreement with the corresponding analytic solutions. Moreover, the DRM is applied to solve problems without analytic solutions. For the cases with $D_1 = D_2$, higher total source at one of boundaries results in higher temperature in the materials. The more curved the internal source g_1 and g_2, the more curved graphs or contour plots of temperature T. However, the total temperature in the domain resulted from curved internal source g_1 and g_2 is smaller from that resulted from the other pair of g_1 and g_2. For the cases with $D_1 \neq D_2$, the higher the thermal conductivity in the lower layer, the lower the temperature in the materials.

References

[1] Z.J. Fu, Q. Xi, W. Chen and A.H.D. Cheng, "A boundary-type meshless solver for transient heat conduction analysis of slender functionally graded materials with exponential variations" *Computers & Mathematics with Applications*, Vol. 76(4), pp. 760 - 773, 2018.

[2] H. Bao, J. Chen, X. Gu and B. Cao, "A review of simulation methods in micro/nanoscale heat conduction," *ES Energy & Environment*, Vol. 1, pp. 16 - 55, 2018.

[3] H.J. Xu, Z.B. Xing, F.Q. Wang and Z.M. Cheng, "Review on heat conduction, heat convection, thermal radiation and phase change heat transfer of nanofluids in porous media: Fundamentals and applications," *Chemical Engineering Science*, Vol. 195, pp. 462 - 483, 2019.

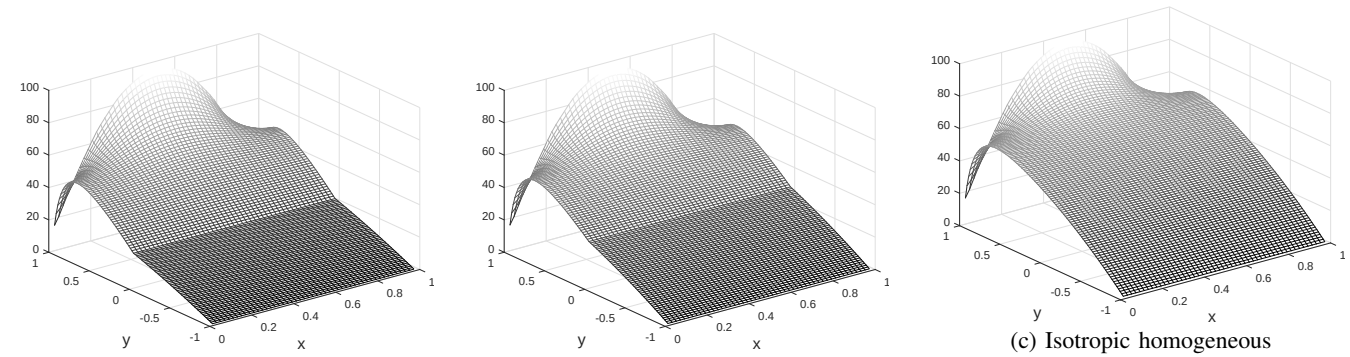

(a) Case A (b) Case B (c) Isotropic homogeneous material

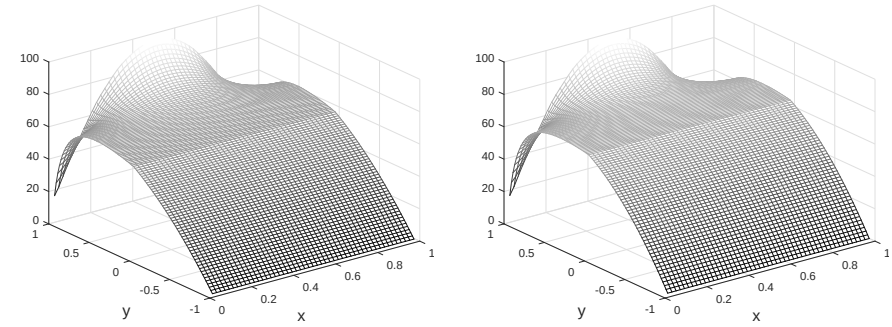

(d) Case C (e) Case D

Fig. 9: Surface plots of T over the region.

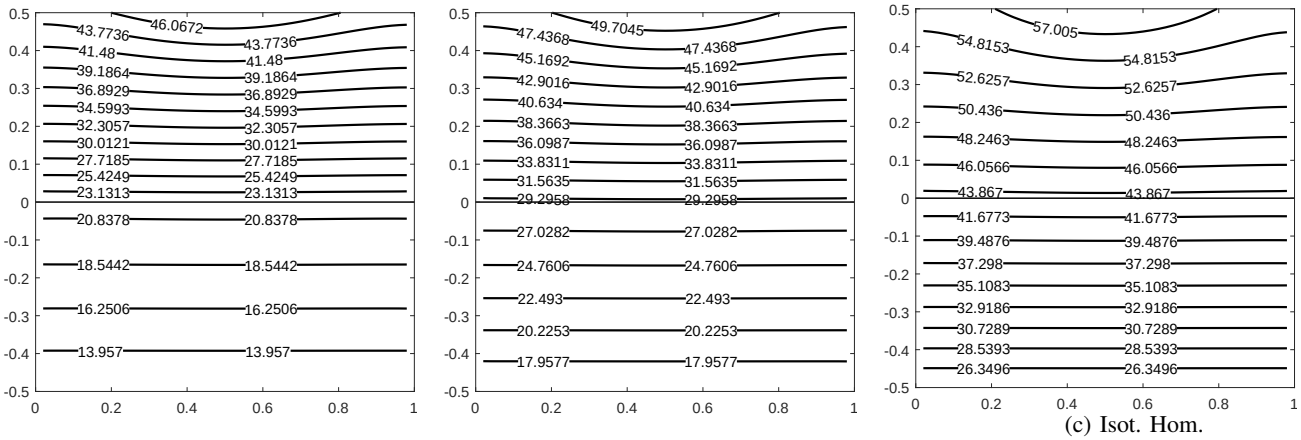

(a) Case A (b) Case B (c) Isot. Hom. material

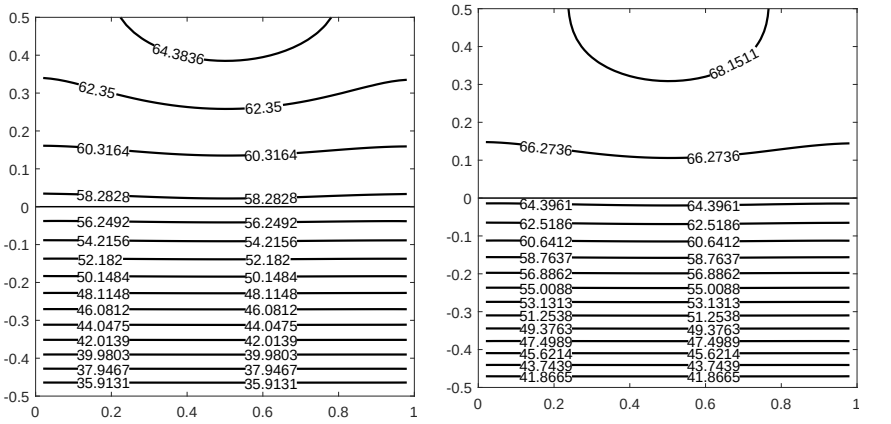

(d) Case C (e) Case D

Fig. 10: Contour plots of T for $-0.5 \leq y \leq 0.5$.

[4] M.I. Azis, I. Solekhudin, M.H. Aswad, S. Hamzah and A.R. Jalil, "A Combined Laplace Transform and Boundary Element Method for Unsteady Laplace Problems of Several Classes of Anisotropic Functionally Graded Materials," *Engineering Letters*, Vol. 29(2), pp. 534 - 542, 2021.
[5] A.A.N. Pramesti, I. Solekhudin and M.I. Azis, "Implementation of Dual Reciprocity Boundary Element Method for Heat Conduction Problems in Anisotropic Solid," *IAENG International Journal of Applied Mathematics*, Vol. 52(1), pp. 122 - 130, 2022.
[6] I. Solekhudin, "Boundary interface water infiltration into layered soils using dual reciprocity methods," *Engineering Analysis with Boundary Elements*, Vol. 119, pp. 280 - 292, 2020.
[7] J. Gao, Y. Feng, W. Guo and L. Jiang, "Nanofluidics in two-dimensional layered materials: inspirations from nature," *Chem. Soc. Rev.*, Vol. 46, pp. 5400 - 5424, 2017.
[8] B.T. Johansson and D. Lesnic, "A method of fundamental solutions for transient heat conduction in layered materials," *Engineering Analysis with Boundary Elements*, Vol. 33(12), pp. 1362 - 1367, 2009.
[9] L. Qiu, F. Wang and J. Lin, "A meshless singular boundary method for transient heat conduction problems in layered materials," *Computers & Mathematics with Applications*, Vol. 78(1), pp. 3544 - 3562, 2019.
[10] S.A. Al-Bayati and L.C. Wrobel, "A novel dual reciprocity boundary element formulation for two-dimensional transient convection–diffusion–reaction problems with variable velocity," *Engineering Analysis with Boundary Elements*, Vol. 94, pp. 60 - 68, 2018.
[11] S.A. Al-Bayati and L.C. Wrobel, "The dual reciprocity boundary element formulation for convection-diffusion-reaction problems with variable velocity field using different radial basis functions," *International Journal of Mechanical Sciences*, Vol. 145, pp. 367 - 377, 2018.
[12] H. Fendoğlu, C. Bozkaya and M. Tezer-Sezgin, "DBEM and DRBEM solutions to 2D transient convection-diffusion-reaction type equations," *Engineering Analysis with Boundary Elements*, Vol. 93, pp. 124 - 134, 2018.
[13] Munadi, I. Solekhudin, Sumardi and A. Zulijanto, "A numerical study of steady infiltration from a single irrigation channel with an impermeable soil layer," *Engineering Letters*, Vol. 28(3), pp. 643 - 650, 2020.
[14] I. Solekhudin, "Suction potential and water absorption from periodic channels in a homogeneous soil with different root uptakes," *Advances and Applications in Fluid Mechanics*, Vol. 20(1), pp. 127 - 139, 2017.
[15] I. Solekhudin, "A numerical method for time-dependent infiltration from periodic trapezoidal channels with different types of root-water uptake," *IAENG International Journal of Applied Mathematics*, Vol. 48(1), pp. 84 - 89, 2018.
[16] I. Solekhudin and K.C. Ang, "A Laplace transform DRBEM with a predictor-corrector scheme for time-dependent infiltration from periodic channels with root-water uptake," *Engineering Analysis with Boundary Elements*, Vol. 50, pp. 141 - 147, 2015.
[17] I. Solekhudin, "Suction potential and water absorption from periodic channels in a homogeneous soil with different root uptake," *Advances and Applications in Fluid Mechanics*, Vol. 20(1), pp. 127 - 139, 2017.
[18] Munadi, I. Solekhudin, Sumardi and A. Zulijanto, "Steady water flow from different types of single irrigation channel," *JP Journal of Heat and Mass Transfer*, Vol. 16(1), pp. 95 - 106, 2019.
[19] I. Solekhudin, D. Purnama, N. H. Malysa and Sumardi, "Characteristic of water flow in heterogenous soils," *JP Journal of Heat and Mass Transfer*, Vol. 15(3), pp. 597 - 608, 2018.
[20] E.L. Albuquerque, P. Sollero and P. Fedelinski, "Dual reciprocity boundary element method in Laplace domain applied to anisotropic dynamic crack problems," *Computers & Structures*, Vol. 81(17), pp. 1703 - 1713, 2003.
[21] A.F. Galvis and P. Sollero, "2D analysis of intergranular dynamic crack propagation in polycrystalline materials a multiscale cohesive zone model and dual reciprocity boundary elements," *Computers & Structures*, Vol. 164, pp 1 - 14, 2016.
[22] C.A.R. Vera-Tudela and J.C.F. Telles, "A numerical Green's function and dual reciprocity BEM method to solve elastodynamic crack problems," *Engineering Analysis with Boundary Elements*, Vol. 29(3), pp. 204 - 209, 2005.
[23] N.Y. Ashar and I. Solekhudin, "A Numerical Study of Steady Pollutant Spread in Water from a Point Source," *Engineering Letters*, Vol. 29(3), pp. 840 - 848, 2021.
[24] I. Solekhudin and K.C. Ang, "A dual-reciprocity boundary element method for steady infiltration problems," *The ANZIAM Journal*, Vol. 54(3), pp. 171 - 180, 2012.
[25] B.I. Yun and W.T. Ang, "A Dual Reciprocity Element Approach for Axisymmetric Nonlinear Time-Dependent Heat Conduction in a Non-homogeneous Solid," *Engineering Analysis with Boundary Elements*, vol. 34(8), pp. 697 - 706, 2010.